PNAS RESEARCH ARTICLE | AGRICULTURAL SCIENCES OPEN ACCESS

Rhomboid-mediated cleavage of the immune receptor XA21 protects grain set and male fertility in rice

Satyam Vergish[a,1,2], Xiaoen Huang[a,1,2], Guiyun Zhang[a,3], Beatriz de Toledo Franceschi[a], Jian-Liang Li[b], Xiao-Xia Wu[a,4], Joana Nuraj[a,5], Jose C. Huguet-Tapia[a], Apekshya Parajuli[a], Xiuhua Chen[c], Ritu Shekhar[d], Dali Liu[a,6], Wu-Ming Xiao[a,7], Shijuan Dou[e], Guo-zhen Liu[e], Erica M. Goss[a,f], Liya Pi[g], Sixue Chen[h,i], Karen E. Koch[j], and Wen-Yuan Song[a,8]

Affiliations are included on p. 10.

Edited by Jan Leach, Colorado State University, Fort Collins, CO; received February 7, 2025; accepted April 9, 2025

To maintain growth and to successfully reproduce, organisms must protect key functions in specific tissues, particularly when countering pathogen invasion using internal defensive proteins that may disrupt their own developmental processes. The rice immune receptor XA21 confers race-specific resistance against *Xanthomonas oryzae* pv. *oryzae*, which causes the deadly disease bacterial leaf blight. Here, we demonstrate that XA21 is cleaved by the rhomboid-like protease OsRBL3b, likely within its transmembrane domain. *OsRBL3b* mRNA transcripts are preferentially expressed in rice spikelets. Rice plants expressing *Xa21* but lacking a functional *OsRBL3b* displayed impaired anther dehiscence and pollen viability, resulting in male sterility and yield reduction with high levels of XA21 protein present in spikelets during anthesis. In leaves, *osrbl3b* mutants expressing XA21 had normal levels of this resistance protein and disease immunity. This balance between reproduction and disease resistance through the specific expression of a rhomboid protease may be key to limiting the detrimental effects of an active immune response and may be useful in future for genetic improvement of crops.

intramembrane protease | innate immune receptor | disease resistance | *Oryza sativa*

Significance

The protection of key developmental processes from the immune system, while allowing the immune system to defend against pathogens, is central for the survival and reproduction of nearly all multicellular organisms. The rice immune receptor XA21 specifies resistance against the bacterial pathogen *Xanthomonas oryzae* pv. *oryzae*. Here, we demonstrate that the rice rhomboid-like protease OsRBL3b controls the steady-state level of XA21 in spikelets and prevents XA21-induced male sterility and yield penalty. In leaves, the *OsRBL3b* gene is expressed at low levels and has little effect on XA21-mediated immunity. Therefore, these results reveal a regulatory mechanism by which rhomboid-mediated proteolysis of a transmembrane domain-containing receptor prevents detrimental impacts of an activated immune system on reproduction in a major food crop.

Plants and animals have evolved multiple defense mechanisms against various and ever-evolving pathogens. In plants, the first line of the active defense system includes cell-surface transmembrane domain (TMD) receptors, known as pattern recognition receptors (PRRs), that detect molecules associated with either microbes or cellular damage and that activate a suite of defense responses called pathogen-triggered immunity (PTI), ultimately resulting in restriction of the proliferation of a wide variety of microbes (1–4). Some pathogens have adapted to survive this line of defense by developing effector proteins capable of inactivating PTI. To defeat this group of pathogens, plants carry hundreds of intracellular receptors in the nucleotide binding domain and leucine-rich repeat (NLR) family that recognize the effectors and induce a second layer of strong defense, known as effector-triggered immunity (ETI) (5). Most disease resistance (*R*) genes identified in plants encode NLRs and confer race-specific resistance to pathogens. However, fitness costs incurred by the expression of *R* genes—even in the absence of pathogens—have been observed (6, 7). Despite the need to balance growth and defense, the molecular mechanisms spatiotemporally controlling immune receptors are not fully understood, especially for the membrane-bound receptors at the posttranslational level.

The *R* gene *Xa21* was originally identified in a Mali accession of African wild rice *Oryza longistaminata* for conferring robust, race-specific resistance to the Gram-negative bacterium *Xanthomonas oryzae* pv. *oryzae* (*Xoo*), the causal agent of bacterial leaf blight disease of rice (8). Through genetic crosses or genetic transformation, *Xa21* was later introduced into cultivated rice varieties (8, 9). *Xa21* encodes a cell-surface receptor-like kinase protein (RLK, XA21), possessing extracellular leucine-rich repeats (LRRs), a single-pass TMD, and an intracellular serine/threonine kinase domain, which is similar in structure to the PRRs discovered in both plants [e.g., FLAGELLIN-SENSING 2 (FLS2) and Elongation Factor Tu Receptor (EFR)] and animals [e.g., Toll-like receptors (TLRs)] (2, 9). XA21 mediates innate immunity by recognizing the sulfated peptide RaxX from the *Xoo* bacterium (10). Interestingly, RaxX shares similarity to phytohormones in the plant Peptide-containing Sulfated tYrosine (PSY) family, which includes eight members (OsPSY1-8) in rice (11). XA21 forms a stable protein complex containing multiple partners, such as the LRR-RLK protein OsSERK2 (rice somatic embryogenesis receptor kinase 2) (12). Importantly, XA21 can act in a temperature-sensitive fashion, with low temperatures priming and high temperatures suppressing XA21-mediated immunity without significantly affecting its abundance (13). Evidence indicates that XA21 can be

[4]Present address: Department of Biological Sciences, College of Biological Sciences and Technology, Yangzhou University, Yangzhou 225009, P. R. China.

[5]Present address: Florida International University Herbert Wertheim College of Medicine, Miami, FL 33199.

[6]Present address: College of Modern Agriculture and Ecological Environment, Heilongjiang University, Harbin 150080, P.R. China.

[7]Present address: National Engineering Research Center of Plant Space Breeding, South China Agricultural University, Guangzhou 510642, P.R. China.

[8]To whom correspondence may be addressed. Email: wsong@ifas.ufl.edu.

This article contains supporting information online at https://www.pnas.org/lookup/suppl/doi:10.1073/pnas.2502025122/-/DCSupplemental.

Published May 30, 2025.

proteolytically cleaved, as observed for three other RLKs: *Lotus japonicus* SYMRK (symbiosis receptor-like kinase), Arabidopsis BAK1/SERK3 (brassinosteroid insensitive 1-associated receptor kinase 1/somatic embryogenesis receptor-like kinase 3), and Arabidopsis CERK1 (chitin elicitor receptor kinase 1) (14–19). We previously hypothesized that proteolytic cleavage might have a role in regulating XA21 levels in an effort to maintain homeostasis (14); however, neither the corresponding proteases nor the biological significance of any such cleavage have been reported.

One mechanism that can modulate membrane-embedded proteins is hydrolysis of residues within their TMDs by intramembrane proteases (20). Rhomboid proteins are intramembrane proteases and comprise the most widely conserved intramembrane protease superfamily, with more than 25,000 members and a presence in nearly all branches of life (20–22). Here, we report that mutations of a rice rhomboid protease gene, *OsRBL3b*, cause increased accumulation of the immune receptor XA21 in the floral spikelet during anthesis and elevated XA21-induced fertility alterations, such as impaired anther dehiscence, reduced pollen viability, and reduced grain set. Our findings highlight a molecular mechanism by which the XA21-mediated response is regulated to avoid detrimental penalties during the development of rice.

Results

Identification and Cellular Localization of OsRBL3b Protein. We previously reported that XA21 confers tolerance to water-deficit stress (23). Our analysis of the RNA-seq data from this study identified *OsRBL3b* (also known as *OsRhmbd17*) as being up-regulated by water-deficit stress in transgenic plants expressing XA21 (XA21 plants) relative to control plants (Dataset S1). The OsRBL3b protein is predicted to contain seven putative TMDs and belongs to the RhoA1 subfamily of plant rhomboid-like proteases (RBLs), with OsRBL3a (also known OsRhmbd7) being the most closely related family member (ref. 24 and *SI Appendix,* Figs. S1 and S2). Phylogenetic analysis indicated that OsRBL3a and OsRBL3b are distinct homologs that likely diverged from a common ancestor that predates *Oryza* divergence from other genera tested (*SI Appendix,* Fig. S2). Topological analysis suggested that OsRBL3b carries catalytic sites located close to the extracellular sides of both TMD4 and TMD6, which would allow the cleavage of substrates at sites near the N termini of these two TMDs (*SI Appendix,* Fig. S1). To identify the subcellular localization of OsRBL3b, we performed green fluorescent protein (GFP) imaging of rice protoplasts transfected with a *GFP-OsRBL3b* construct expressed from a double cauliflower mosaic virus (CaMV) *35S* promoter. OsRBL3b was mainly detected in the plasma membrane as evidenced by its colocalization with the FM4-64-stained plasma membrane in the transfected rice cells (*SI Appendix,* Fig. S3). In addition to the plasma membrane, GFP signals were also detected in an unknown subcellular compartment(s) of some cells, which appeared to increase with prolonged incubation time of the protoplasts. Since XA21 also resides in the plasma membrane (25, 26), we hypothesized that XA21 might be a substrate of OsRBL3b.

Preferential Expression of *OsRBL3b* in Spikelets. The expression of *OsRBL3b* and the other rice *RhoA1* genes were analyzed in the microarray data previously published in RiceXpro (http://ricexpro.dna.affrc.go.jp/). *OsRBL3b* transcripts accumulated highly in spikelets, but declined rapidly after anthesis (*SI Appendix,* Fig. S4 and Dataset S2). In contrast, *OsRBL3b* mRNAs were markedly less abundant in the leaves at both the vegetative and reproductive stages (Dataset S2). Notably, five other rice *RhoA1* genes also showed largely distinct spatiotemporal expression, including in the leaf sheath, root, stem, inflorescence, anther, pistil, lemma/palea, ovary, embryo, and/or endosperm, but still low transcript levels in the leaf blades, which is the major site for plant–microbe interactions (*SI Appendix,* Fig. S4 and Dataset S2). For example, the expression patterns of *OsRBL3a* and *OsRBL3b* largely differed with *OsRBL3a* preferably expressed in roots (*SI Appendix,* Fig. S4 and Dataset S2). Among the genes encoding the other three rice RhoA members (OsRBL3c, OsRBL3d, and OsRBL3e) that are closely related to OsRBL3b (*SI Appendix,* Fig. S2), *OsRBL3c* was highly expressed in leaf sheath and moderately expressed in stem and in lemma and palea (*SI Appendix,* Fig. S4 and Dataset S2). *OsRBL3e* expression could be found in stem, root, ovary, lemma, and palea. In contrast, *OsRBL3d* was expressed in most rice tissues. These differences in expression sites could be explained by the limited nucleotide sequence identities (36.8 to 43.9%) in the 5′ flanking regions (2-kb) of these genes (Dataset S3). These findings, together with our previous thoughts on XA21 cleavage, led to the hypothesis that OsRBL3b functions in the rice spikelet to minimize accumulation of the immune receptor for the maintenance of physiological homeostasis in this vulnerable tissue (14).

To test our hypothesis, we used RT-qPCR to measure the expression of *OsRBL3b* in a previously characterized transgenic line (U0-137) carrying a construct encoding an N-terminal c-Myc-tagged XA21 (Myc-XA21) expressed from its native promoter at a relatively low level (*Myc-Xa21*^{L}) (14). We detected high *OsRBL3b* transcript levels specifically in spikelets during floral development, but low levels in rice leaf tissues at distinct developmental stages (Fig. 1*A*). We then confirmed that the XA21 protein is readily detectable in the spikelet of this line as well as another previously characterized line (*Myc-Xa21*^{H}, also known as 4021-3) expressing the same fusion protein at a higher level of XA21, due to a distinct transformation event (Fig. 1 *B* and *C* and ref. 14). In this study, we focused on the role of *OsRBL3b* during flower and grain development in rice plants carrying XA21. The function of the OsRBL3b protease in response to water-deficit stress will be studied separately.

OsRBL3b Mediates Cleavage of XA21 in *Nicotiana benthamiana*. To determine whether XA21 can be cleaved by OsRBL3b, we coexpressed constructs encoding epitope-tagged XA21 (Myc-XA21-FLAG) (Fig. 2*A*) and OsRBL3b (HA-OsRBL3b) proteins in *N. benthamiana* grown under low temperature conditions [24/21 °C (light/dark)]. We repeatedly observed cleavage of XA21 in the infiltrated leaf tissues in an OsRBL3b-dependent manner (Fig. 2 *B* and *C* and *SI Appendix,* Fig. S5). Mutation of the catalytic serine residue of OsRBL3b (Ser-187) to alanine abolished the cleavage (Fig. 2*B*). The rhomboid protease OsRBL3a was unable to efficiently cleave XA21 (Fig. 2*C* and *SI Appendix,* Fig. S5). These results confirm that XA21 is a substrate of OsRBL3b.

OsRBL3b Controls the Steady-State Levels of XA21 in Rice Spikelets. We then determined whether OsRBL3b influences XA21 accumulation in rice. We generated homozygous *osrbl3b* mutants [*osrbl3b-1* (p.Trp111ThrfsTer121) and *osrbl3b-2* (p.Asp112GlufsTer116)] in the bacterial blight susceptible line *O. sativa* ssp. *japonica* var. Taipei 309 (TP309) using CRISPR/Cas9-mediated gene editing. The mutants we obtained carried frameshift mutations resulting in premature termination of translation; if any protease accumulated, these truncated OsRBL3b products lacked the catalytic Ser-187 residue (*SI Appendix,* Fig. S6). Thus, they likely harbored loss-of-function alleles of *OsRBL3b*. As a control, we obtained wild-type siblings (WT^{sib}) segregated from the heterozygous *osrbl3b-1*

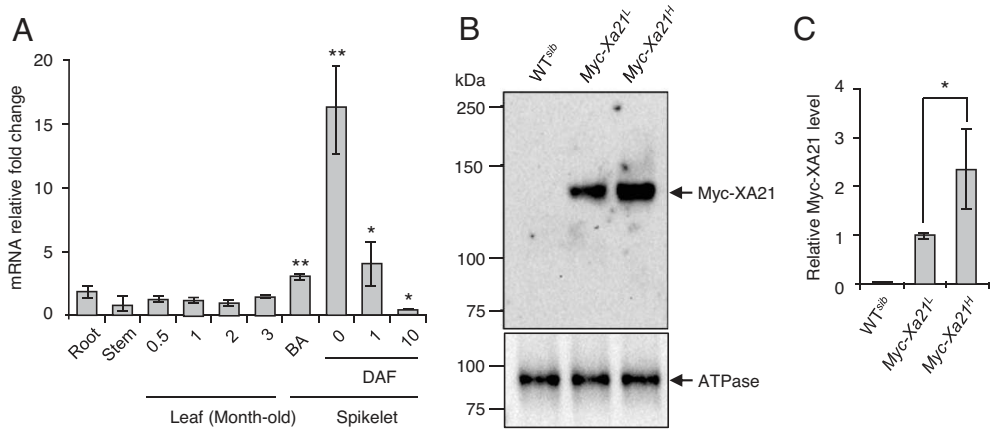

Fig. 1. Expression of *OsRBL3b* and accumulation of XA21 in rice spikelets at anthesis. (*A*) *OsRBL3b* is preferentially expressed in spikelets. Levels of mRNA were quantified by RT-qPCR using the *Myc-Xa21*^{L} line. Results were normalized to the expression of the housekeeping genes *UBIQUITIN5* and *ACTIN*. Expression levels in the indicated tissues were expressed relative to those of 2-mo-old leaves, which were arbitrarily set to 1 unit. Values are means ± SD of three biological replicates, each with three technical replicates. DAF, days after flowering. BA, before anthesis. (*B*) Accumulation of Myc-XA21 protein in spikelets. Myc-XA21 protein levels were determined in the indicated lines by immunoblot using an anti-Myc antibody, with ATPase levels as loading controls. WT^{sib} lacking XA21 is a negative control. Spikelets from more than three plants per line were used for protein extraction. (*C*) Quantification of Myc-XA21 from (*B*). This immunoblotting was repeated three times with similar results (all replicates in this study are shown in *SI Appendix*). In each experiment, the Myc-XA21 protein level was normalized against the ATPase level. The Myc-XA21 protein level in *Myc-Xa21*^{L} was set to 1.0 as references for calculating the relative level of Myc-XA21 in *Myc-Xa21*^{H}. Statistical analyses were performed using Student's *t*-test. Asterisks denote statistically significant differences (**P* < 0.05, ***P* < 0.01).

OsRBL3b line for characterization. To generate XA21 plants with *OsRBL3b* mutations, we individually crossed *osrbl3b-1* and *osrbl3b-2* to *Myc-Xa21*^{L}. F1 plants were self-fertilized to produce progeny. We identified homozygous *osrbl3b-1 Myc-Xa21*^{L} and *osrbl3b-2 Myc-Xa21*^{L} lines in the F4 generation by hygromycin selection for *Myc-Xa21* and by PCR genotyping followed by sequencing for the *osrbl3b* mutations. In addition, we transformed the same CRISPR/Cas9 construct into *Myc-Xa21*^{H} and recovered one biallelic mutant line, *osrbl3b-b* [p.(Trp111ThrfsTer121);(Asp112GlyfsTer116)] *Myc-Xa21*^{H}.

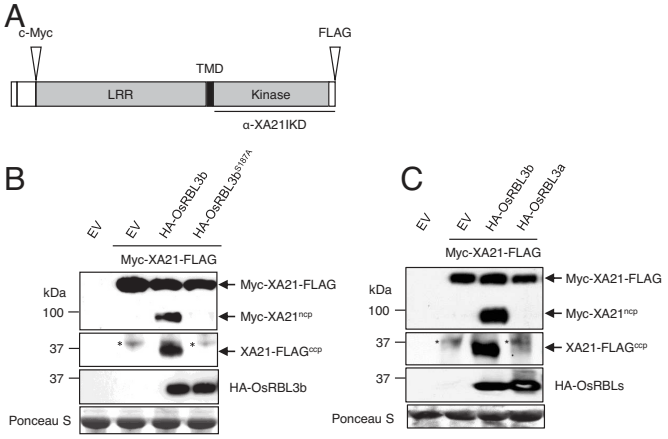

Fig. 2. OsRBL3b mediates cleavage of XA21 in *N. benthamiana*. (*A*) Diagram of the *Xa21* construct used for the cleavage assay in *N. benthamiana*. LRR, leucine-rich repeat domain; TMD, transmembrane domain. c-Myc and 3xFLAG epitope tags were fused to XA21 for detecting the N terminus and C-terminus of the protein, respectively. The intracellular kinase domain (IKD) used to generate the α-XA21IKD antibody is indicated by the black horizontal line. (*B*) Cleavage of XA21 depends on active OsRBL3b. Constructs encoding the indicated proteins were coexpressed in *N. benthamiana*. OsRBL3b^{S187A} is mutated in the catalytically essential residue Ser187. Total protein extracts were subjected to immunoblot analysis using an anti-Myc antibody, anti-XA21IKD, and anti-HA antibody, respectively. EV, empty vector. Asterisks indicate nonspecific cleavage products. Ponceau S staining of Rubisco large subunit was used as loading control. Ncp, N-terminally cleaved product; ccp, C-terminally cleaved product. (*C*) OsRBL3b specifically mediates XA21 cleavage. OsRBL3a is closely related to OsRBL3b (*SI Appendix*, Fig. S2). Protein samples in *B* and *C* were prepared independently.

Consistent with the in vitro cleavage presented above (Fig. 2), XA21 protein levels were repeatedly higher in the spikelets of all *osrbl3b* mutant lines than in the wild type at anthesis (Fig. 3 *A*, *B*, *D*, and *E*). RT-qPCR analysis showed that *Xa21* transcripts accumulated to comparable levels in the spikelets of *osrbl3b Myc-Xa21* and *Myc-Xa21* lines (Fig. 3 *C* and *F*). Based on three independent *osrbl3b* mutant lines, these findings indicate that OsRBL3b negatively regulates steady-state accumulation of the XA21 protein in spikelets. In leaves, regardless of the presence of a functional *OsRBL3b*, XA21 abundance was not obviously affected (Fig. 3 *G* and *H*).

***OsRBL3b* Is Required for Grain Set in Rice Carrying the XA21 Immune Receptor.** The *osrbl3b-b Myc-Xa21*^{H} mutant was completely sterile in all seasons over seven years of growth in a green house without exposure to *Xoo* (*Xoo* is a quarantine pathogen in the United States) (Fig. 4 *A* and *B*). The *osrbl3b Myc-Xa21*^{L} lines showed markedly reduced grain set when grown during low-temperature seasons (i.e., some springs or falls) in a greenhouse or a temperature-controlled growth chamber at low temperatures [28/24 °C (light/dark)]. The average rates of grain-set for the *osrbl3b Myc-Xa21*^{L} was ~30 to 40% compared to >70 to 97% for the controls (WT^{sib}, *osrbl3b-1*, *osrbl3b-2*, and *Myc-Xa21*^{L}) (Fig. 4 *C*–*E*). In summer, the grain-setting rates of *osrbl3b Myc-Xa21*^{L} plants were similar to those of the controls (*SI Appendix*, Fig. S7). These observations are in line with the temperature-sensitive nature of XA21 signaling (13). The *osrbl3b-2* line and *Myc-Xa21*^{L} line showed slightly lower grain-setting rates than did WT^{sib} or *osrbl3b-1* when grown in a growth chamber at the same low temperatures (Fig. 4*E*). Apart from the fertility defect, *osrbl3b Myc-Xa21*^{L} plants grew normally (Fig. 4*D*). These findings indicate that *OsRBL3b* is required for normal grain setting in plants carrying XA21 and that the influence of XA21 on rice grain set is dose dependent.

We inoculated 2-wk-old seedlings of *osrbl3b Myc-Xa21*^{L} with the incompatible *Xoo* strain PXO99^{A}. As expected, *OsRBL3b* mutations did not significantly affect XA21-mediated resistance as compared to plants carrying *Myc-Xa21*^{L} (Fig. 4 *F* and *G*). In contrast, the susceptible control line WT^{sib} (lacking *Xa21*) was killed by bacterial infection at the seedling stage (Fig. 4*H*).

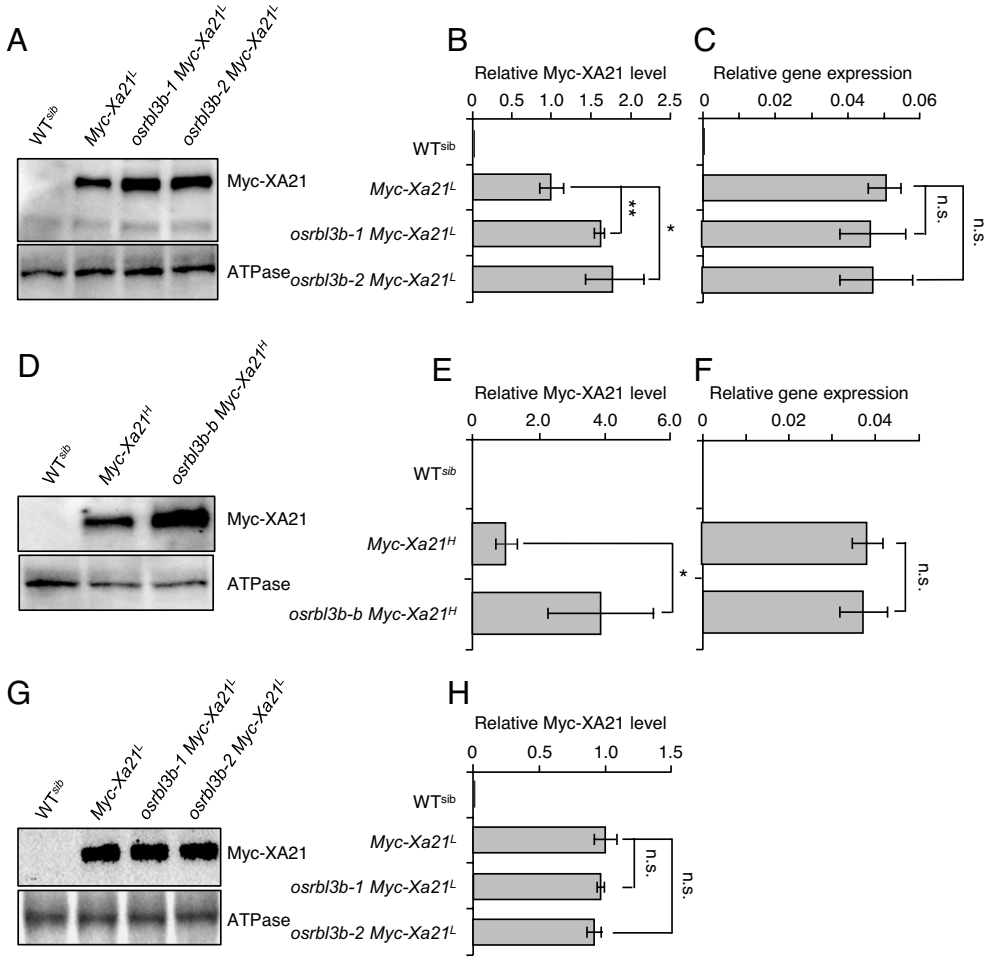

Fig. 3. *OsRBL3b* specifically controls the steady-state levels of XA21 in rice spikelets at anthesis. (*A*) Accumulation of Myc-XA21 protein in the spikelet of WT^{sib}, *Myc-Xa21*^{L}, and the *osrbl3b Myc-Xa21*^{L} mutants, determined by immunoblot analysis using an anti-Myc antibody and anti-ATPase as a loading control. Spikelets used for the experiment were collected from fresh plants. (*B*) Quantification of Myc-XA21 protein from *A*. (*C*) Relative *Myc-Xa21* transcript levels, quantified by RT-qPCR, in spikelets of the lines shown in *A*. (*D*) Accumulation of Myc-XA21 protein in the spikelet of the *osrbl3b-b Myc-Xa21*^{H} and the *Myc-Xa21*^{H} lines. Spikelets used for the experiment were harvested from plants maintained by continuous ratooning. (*E*) Quantification of Myc-XA21 protein from *D*. (*F*) Relative *Myc-Xa21* transcript levels, quantified by RT-qPCR, in spikelets of the *osrbl3b-b Myc-Xa21*^{H} and *Myc-Xa21*^{H} lines. (*G*) Myc-XA21 protein accumulation in leaves of WT^{sib}, *Myc-Xa21*^{L}, and *osrbl3b Myc-Xa21*^{L}. (*H*) Quantification of Myc-XA21 protein from *G*. Myc-XA21 protein levels in *B*, *E*, and *H* were first normalized with ATPase levels. For each experiment, the Myc-XA21 protein level in *Myc-Xa21*^{L} was set to 1.0 as references for calculating the relative level of protein Myc-XA21 in the other lines. Results in *C* and *F* were normalized relative to levels of mRNAs for *UBIQUITIN 5* and *ACTIN*. Values are means ± SD of three biological replicates, each with three technical replicates. The immunoblot analyses were repeated three times with similar results. WT^{sib} (lacking *Xa21*) was used as a negative control for Myc-XA21 protein and *Myc-Xa21* transcript abundance. Values in *B*, *E*, and *H* are the means ± SD (n = 3, biological replicates). Spikelets from more than three plants per line were used for protein or RNA extraction. Statistical analyses were performed using Student's *t*-test. Asterisks indicate statistically significant differences (*P < 0.05, **P < 0.01); n.s., not statistically significant difference.

***OsRBL3b* Is Required for Pollen Viability and Dehiscence When XA21 Is Present in Rice.** To understand the physiological mechanisms underlying the impaired fertility of the *osrbl3b Myc-Xa21* lines, we first examined the starch contents of their pollen grains, a commonly used marker for pollen viability. The sterile line *osrbl3b-b Myc-Xa21*^{H} produced only ~18% viable pollen grains (Fig. 5*A*). Under low-temperature conditions, the partially sterile *osrbl3b Myc-Xa21*^{L} mutants also produced fewer viable pollen grains (~38% for *osrbl3b-1 Myc-Xa21*^{L} and ~34% for *osrbl3b-2 Myc-Xa21*^{L}) relative to the more fertile controls (>82% for WT^{sib}, *osrbl3b-1*, *osrbl3b-2,* and *Myc-Xa21*^{L}) (Fig. 5*B*). These findings indicate that XA21 impairs starch accumulation in pollen grain in a dose-dependent manner.

We also tested whether the female organ of *osrbl3b-b Myc-Xa21*^{H} remains functional by crossing the sterile *osrbl3b-b Myc-Xa21*^{H} (pollen recipient) with the wild-type TP309, which can supply functional pollen. We found that the mutant was able to set grains, suggesting that sterility of *osrbl3b-b Myc-Xa21*^{H} is mainly due to defects in its male organ. Since the sterile *osrbl3b-b Myc-Xa21*^{H} produced some viable pollen grains, we then examined the ability of its anthers to release pollen at anthesis (anther dehiscence), which is essential for pollination and fertilization (27). None of the spikelets dissected from the *osrbl3b-b Myc-Xa21*^{H} mutant dehisced 2 h after anthesis (HAA; n > 200) or even 10 d after flowering (DAF; n > 30) (Fig. 5*C*). Pollen was still detectable in the anthers of this line. In agreement with the indehiscent anthers, we did not observe pollen grains on the stigmas of the dissected spikelets from the *osrbl3b-b Myc-Xa21*^{H} mutant. Thus, anther indehiscence alone could explain the sterility of *osrbl3b-b Myc-Xa21*^{H} plants, although we cannot exclude the presence of other defects that also affect the fertility of the mutant.

We then examined the partially sterile lines *osrbl3b Myc-Xa21*^{L} and their controls (WT^{sib}, *osrbl3b-1*, *osrbl3b-2*, and *Myc-Xa21*^{L}) grown in the growth chamber at a 28 °C day-light temperature. Among more than 100 randomly chosen spikelets, indehiscent ones were rare in the controls (≤5%) (Fig. 5 *D* and *E*). By contrast, ~25 to 28% of spikelets from the *osrbl3b Myc-Xa21*^{L} lines were indehiscent at 2 HAA. Higher percentages of weakly dehiscent

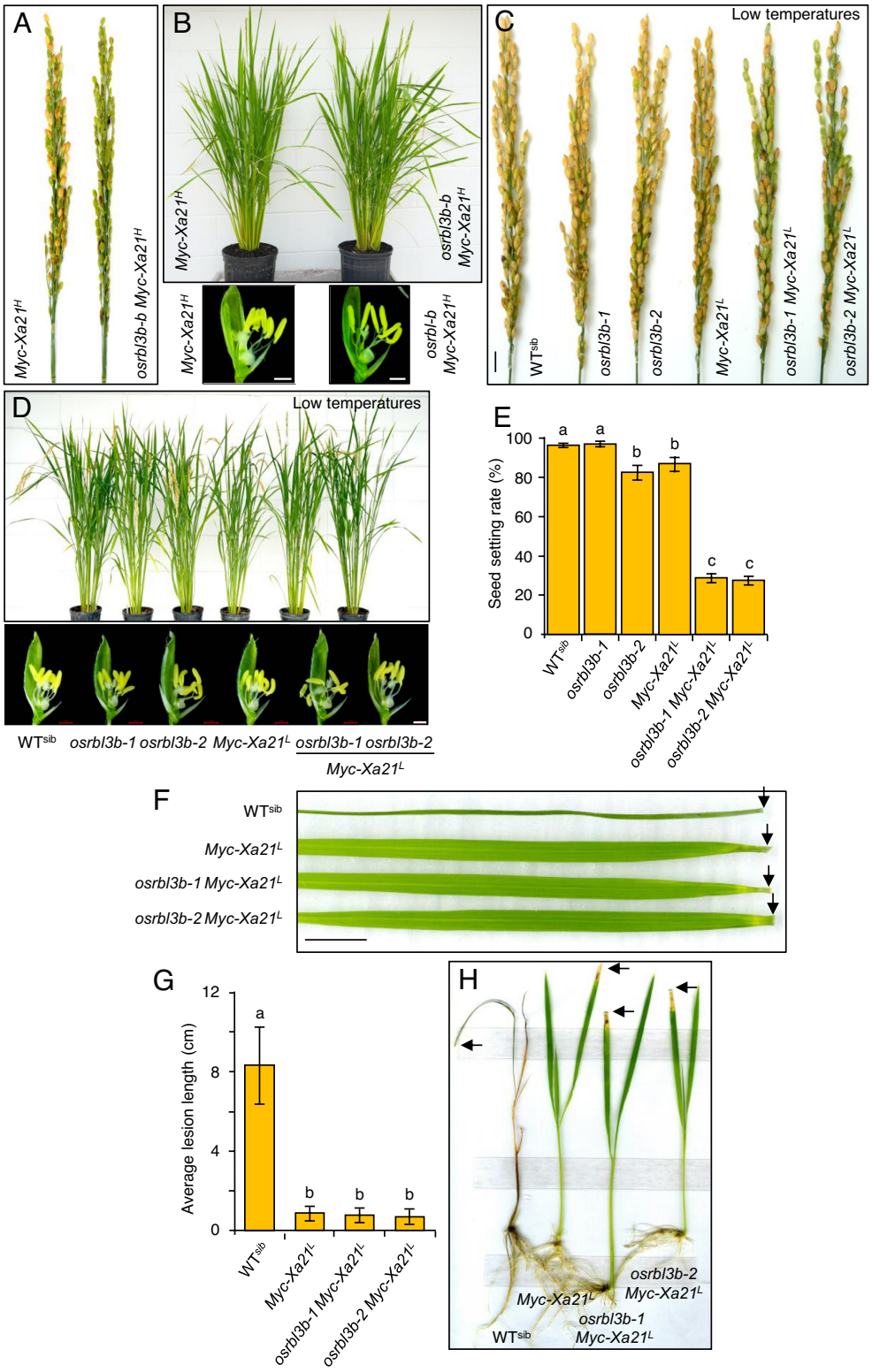

Fig. 4. Mutation of OsRBL3b decreases grain-set but retains resistance in an XA21-dependent manner. (*A*) Panicle phenotypes of the *Myc-Xa21*^{H} line and the sterile *osrbl3b-b Myc-Xa21*^{H} mutant line. (*B*) Phenotypes of mature plants (*Upper*) and floral structure (*Lower*) of the indicated lines in *A*. (Scale bars, 1 mm.) Materials used for the experiments described in *A* and *B* were harvested from plants maintained by continuous ratooning in a greenhouse. (*C*) Panicle phenotypes of control lines and *osrbl3b Myc-Xa21*^{L} mutants grown in a temperature-controlled growth chamber at low temperature, showing lower fertility. (Scale bar, 1 cm.) (*D*) Phenotypes of mature plants (*Upper*) and florets (*Lower*) of the indicated lines in *C*. (Scale bar, 1 mm.) (*E*) Grain-setting rates of *osrbl3b Myc-Xa21*^{L} mutants and their controls. Values are shown as the mean ± SD from five independent plants with two sampled panicles each. Statistical analyses were performed using the Tukey–Kramer honestly significant difference test. Different letters indicate statistically significant differences ($P < 0.05$). This experiment was repeated two times in different seasons with similar results. (*F*) XA21 confers normal resistance in the *osrbl3b* mutant background. Indicated lines were inoculated with the *Xoo* strain PXO99^{A} by the leaf-clipping method. Inoculated leaves from the indicated lines showing lesion development at 12 days post inoculation (dpi). Arrows indicate the inoculation sites. (*G*) Lesion length was scored at 12 dpi. Each data point represents 17 inoculated leaves. Values are means ± SD. Statistical analyses were performed using the Tukey–Kramer honestly significant difference test. Different letters indicate statistically significant differences ($P < 0.05$). This experiment was repeated three times with similar results. (*H*) Rice seedlings carrying *Xa21* survive *Xoo* infection regardless of the presence of a functional *OsRBL3b*. The photograph was taken 5 wk post inoculation. Arrows indicate the inoculation sites. Similar results were obtained from 10 inoculated individuals

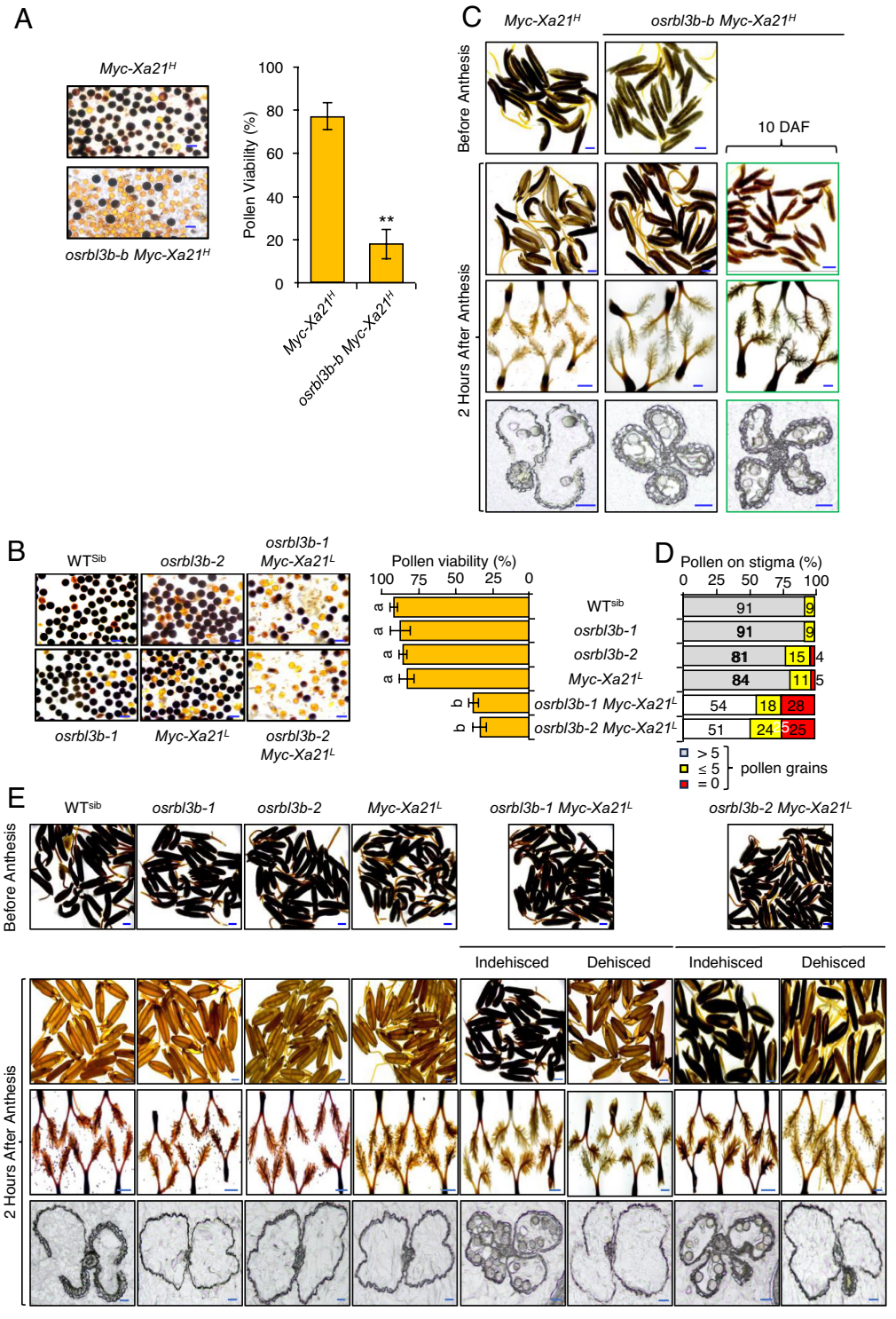

Fig. 5. Mutation of *OsRBL3b* impairs pollen viability and anther dehiscence in an XA21-dependent manner. (*A*) *osrbl3b-b Myc-Xa21*^{H} mutants display lower starch accumulation in their pollen grains. I_2^-KI-stained pollen grains from *Myc-Xa21*^{H} and *osrbl3b-b Myc-Xa21*^{H} lines. Pollen viability was quantified based on the number of stained pollen grains (dark color) relative to the total pollen counted. Values are means ± SD, n = 3 (three independent samplings). Statistical analysis was performed using Student's *t*-test. Asterisks indicate a statistically significant difference (**$P < 0.01$). This experiment was repeated two times with similar results. (*B*) *osrbl3b Myc-Xa21*^{L} mutants display lower starch accumulation in their pollen grains. (*Left*) I_2^-KI-stained pollen grains from *osrbl3b Myc-Xa21*^{L} and the indicated control lines grown in a lower-temperature growth chamber before anthesis. (*Right*) Pollen quantified as above. Values are means ± SD (n = 3). Statistical analysis was performed using the Tukey–Kramer honestly significant difference test. Different letters indicate statistically significant differences ($P < 0.05$). (*C*) (*Top 2 rows*) I_2^-KI staining of pollen grains in anthers of the indicated lines before and after anthesis. (*Third row*) Pollen grains on the stigmas of the indicated lines after anthesis. This experiment was repeated two times with similar results. (*Bottom row*) Cross-sections of anthers from the indicated lines after anthesis. Scale bars in *A* and *B* indicate 500 μm (*rows* 1, 2, and 4) or 50 μm (*row 3*). Materials used for the experiments described in this figure were harvested from plants maintained by continuous ratooning in a greenhouse. (*D*) *osrbl3b* mutations impaired anther dehiscence in the *osrbl3b Myc-Xa21*^{L} line. The graph shows the distribution of dehiscent and indehiscent spikelets among more than 100 random flower samples chosen from five individual plants of each indicated line. (*E*) Morphology of dissected spikelets from the indicated lines. (*Top 2 rows*) I_2^-KI staining of pollen grains in anthers of the indicated lines before anthesis and 2 h after anthesis. (*Third row*) Presence or absence of pollen grains on the stigmas of the indicated lines after anthesis. Both dehisced and indehiscent anthers were shown. This experiment was repeated two times with similar results. (*Bottom row*) Cross-sections of anthers from the indicated lines after anthesis. [Scale bars, 500 μm (*rows* 1, 2, and 4) or 50 μm (*row* 3).]

spikelets (defined as ≤5 pollen grains/stigma) were also observed from the *osrbl3b Myc-Xa21*^{L} lines compared to the controls. Collectively, our findings demonstrate that impaired anther dehiscence was a major reason for reduced grain setting in these two mutants, although additional fertility defects (e.g., reduced pollen viability) might also contribute to the phenotype.

Downregulation of Jasmonic Acid (JA) Responsive and Signaling Genes and Upregulation of *NLR* Genes in the Sterile *osrbl3b-b Myc-Xa21*^{H} Spikelets. To gain insights into the indehiscence observed in *osrbl3b-b Myc-Xa21*^{H}, we performed RNA-seq analysis on spikelets at anthesis from the sterile *osrbl3b-b Myc-Xa21*^{H} and fertile *Myc-Xa21*^{H} lines grown in the greenhouse during summer (optimal for rice growth). A total of 6,331 differentially expressed genes (DEGs) were identified between these two lines using an FDR (False Discovery Rate) value of <0.05 and $\log_2$FC cut-off criteria of >1 and <−1. Altered expression of genes of interest included nine JA-related genes from distinct families and 78 *NLR* genes.

The nine downregulated JA-responsive and JA-signaling genes in *osrbl3b-b Myc-Xa21*^{H} (Fig. 6*A*) were those encoding five JASMONATE ZIM DOMAIN (JAZ) transcriptional repressors (28–30), the CORONATINE INSENSITIVE1a (COI1a) JA receptor (31, 32) and the transcription factors OsbHLH148 (33), RERJ1 (34), and OsWRKY71 (35). The downregulation of seven of these genes with RPKM (reads per kilo base per million mapped reads) values >1 was verified by qRT-PCR analysis (Fig. 6*B*). JA signaling has been implicated in positively regulating pollen development and anther dehiscence in plants (36). Of note, none of the genes encoding the other JA receptors (i.e., OsCOI1b and OsCOI2) or the other JAZ repressors identified in rice were misregulated in the anther indehiscent line (Fig. 6*A*). These results provide a link between compromised expression of JA-responsive and JA-signaling genes and the sterile phenotype of the *osrbl3b-b Myc-Xa21*^{H} mutant during anthesis.

Among the 473 genes annotated as NLR receptors in the rice reference genome from variety Nipponbare (37), 399 were detected in our RNA-seq analysis. Interestingly, 66 of these genes were found to be significantly upregulated in the sterile *osrbl3b-b Myc-Xa21*^{H} spikelets (Fig. 6*C*), while only 12 *NLRs* were downregulated. These findings demonstrate that a large number of *NLR* genes are transcriptionally activated in the *osrbl3b-b Myc-Xa21*^{H} mutant spikelets.

OsRBL3b Can Cleave Noncanonical TMDs of a Subset of Plant RLKs. Canonical TMDs contain predominantly hydrophobic amino acids to maintain an α-helical structure. Noncanonical TMDs with helix-breaking residues (e.g., proline and glycine) at their N-terminal half are often rhomboid substrates, and the presence of proline and glycine residues has been used as a criterion to predict rhomboid cleavage targets (22, 38). XA21 possesses two prolines, Pro-652 and Pro-655, in this region (*SI Appendix,* Fig. S8*A*). Replacing Pro-652 with the hydrophobic residue leucine slightly decreased the cleavage of XA21 by OsRBL3b, while changing Pro-655 to leucine markedly compromised the cleavage (*SI Appendix,* Fig. S8 *B* and *C*). Mutation of both Pro-652 and Pro-655 to leucine residues fully abolished cleavage. Helix-breaking proline and glycine residues are also present in the N-terminal half of many other TMD proteins. For instance, helix-breaking residues were found in 625 of the 786 predicted rice RLKs and 340 of 599 Arabidopsis RLKs (*SI Appendix,* Fig. S8*A* and Datasets S4 and S5). These findings indicate that noncanonical TMDs with intrinsically unstable helices are widely present in plant RLKs.

We tested whether OsRBL3b also cleaves other noncanonical TMDs using an alkaline phosphatase (AP)-based colorimetric assay (22). The TMDs of seven well-studied Arabidopsis RLKs were individually fused in-frame with the C-terminus of AP containing an N-terminal signal peptide, allowing the expressed fusion protein to be localized to the plasma membrane. Rhomboid-mediated cleavage of a TMD will result in the release and accumulation of AP in the extracellular medium, which can be detected by a colorimetric assay. In mammalian HEK 293 cells coexpression of OsRBL3b with the XA21TMD released the AP but not with the uncleavable mutant XA21TMD$^{P652L,\ P655L}$ (*SI Appendix,* Fig. S8*D*). Consistent with the cleavage data from the *N. benthamiana*-based system (Fig. 2), OsRBL3b hydrolyzed XA21TMD, but not XA21TMD$^{P652L,\ P655L}$. Furthermore, the catalytically deficient mutant OsRBL3b^{S187A} failed to cleave the XA21TMD (*SI Appendix,* Fig. S8*D*).

As shown in *SI Appendix,* Fig. S8*D*, OsRBL3b was found to cleave the TMDs of several other tested plant receptor-like kinases. The OsRBL3b cleaved receptor kinase AtBRI1 and its coreceptor AtBAK1/AtSERK3, both involved in perceiving the steroid hormone brassinolide (BR) during cell elongation (39–42). The TMDs of AtEFR, AtCERK1, and AtSERK2 were also cleaved by OsRBL3b. RLK–SERK complexes are a common theme in plant signaling related to hormone and immune responses (43, 44). Overaccumulation of AtBAK1/AtSERK3 in Arabidopsis causes autoimmune cell-death and developmental defects, such as growth arrest and reduced grain production (18, 19). Under our conditions, OsRBL3b failed to cleave the TMDs of AtFLS2 and AtLYK5, which both act as immune receptors (45, 46). From this assay, we can conclude that OsRBL3b and its plant orthologs are likely to cleave multiple RLKs, but one protease does not cleave all RLKs.

Discussion

To detect the infection of pathogens, plants rely on the organism-wide expression of genes encoding immune receptors (3). This constitutive monitoring may incur physiological costs to the plants at cellular sites or development stages that are sensitive to the accumulation and function of immune receptors. In rice, the bacterial pathogen *Xoo* mainly causes disease symptoms in leaves, but the immune receptor XA21 is also detectable in the spikelets at anthesis, where *OsRBL3b* is preferentially expressed. We found that the rhomboid-like protease encoded by *OsRBL3b* cleaves XA21 in vitro and controls the steady-state level of the immune receptor in vivo. We propose that XA21 drastically reduces fertility in a quantitative manner via impairment of floret functions, including anther dehiscence and pollen viability (*SI Appendix,* Fig. S9). In this model, OsRBL3b activity prevents the excessive accumulation of XA21 over a level that would otherwise interfere with the function of reproductive organs, thus decreasing fertility. In leaves, *OsRBL3b* transcript levels are low throughout development, and OsRBL3b has little influence on XA21 accumulation, which ensures optimal host immunity at the main entry site of *Xoo*.

This model raises the question of how an immune receptor with potentially high fitness costs might have evolved in rice. In fact, when *Xa21* was introgressed into *O. sativa*, low seed set would have caused the genotype to be discarded as unusable. OsRBL3b-mediated proteolysis, as described here, represents a balancing mechanism by which the negative effects of XA21 are largely controlled. The species from which *Xa21* was originally discovered, *O. longistaminata*, also contains an ortholog of OsRBL3b (*SI Appendix,* Fig. S2). However, unlike domesticated and many other wild rice accessions, *O. longistaminata* is a perennial species that can propagate via strong rhizomes in spite of its poor seed setting rate (47). Therefore, in *O. longistaminata*, any potential decrease in fertility caused by *Xa21* might have a

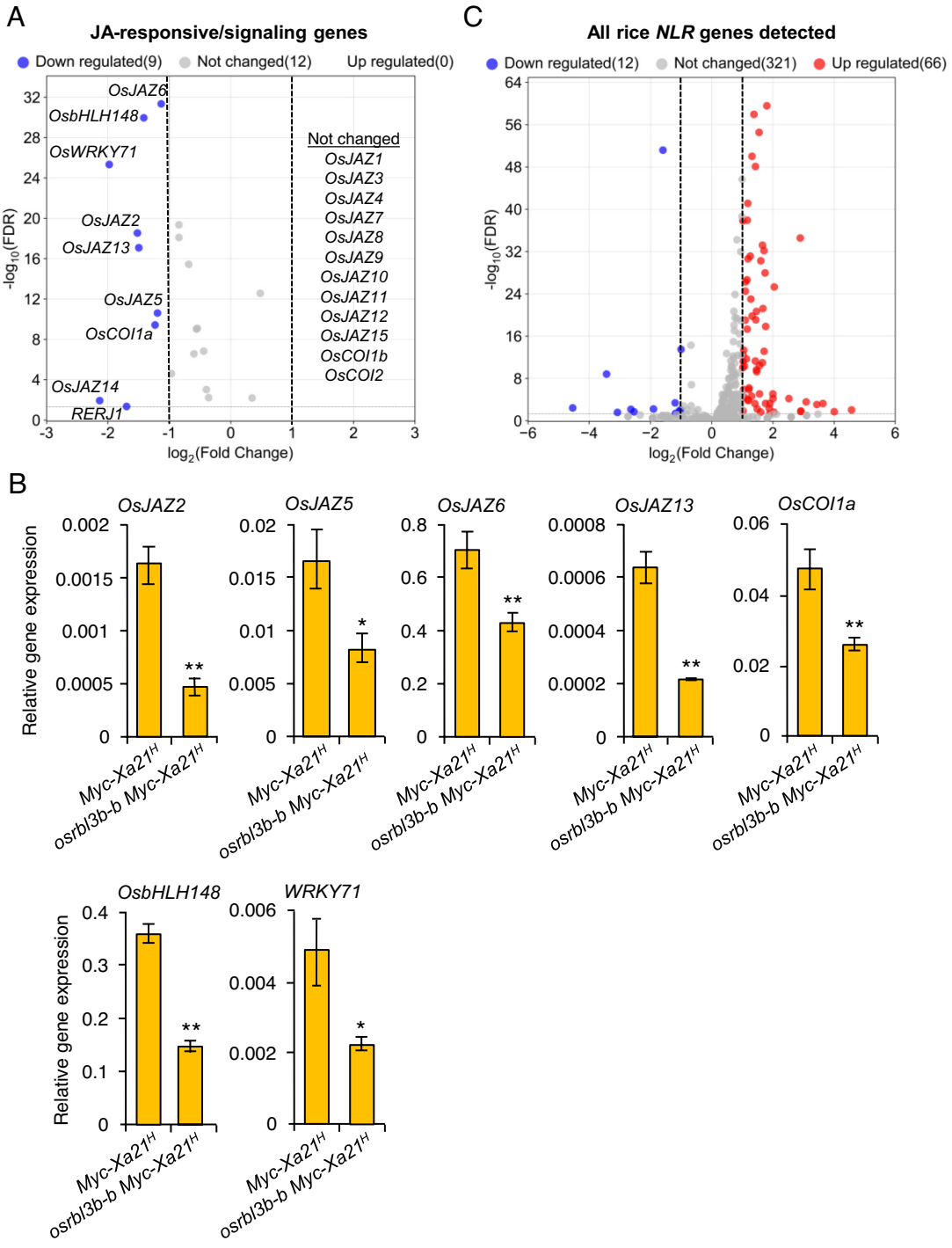

Fig. 6. Down-regulation of JA-responsive and JA-signaling genes and upregulation of defense-related genes in the indehiscent *osrbl3b-b Myc-Xa21*^{H} spikelets relative to the dehiscent *Myc-Xa21*^{H} spikelets at anthesis as detected by RNA-seq analysis. (*A*) RNA-seq volcano plot showing downregulation of a set of JA-responsive and JA-signaling genes. (*B*) Relative transcript levels of the JA-responsive and JA-signaling genes in *A* with RPKM (reads per kilo base per million mapped reads) >1, quantified by RT-qPCR, in spikelets of lines *Myc-Xa21*^{H} and *osrbl3b-b Myc-Xa21*^{H}. Results were normalized relative to levels of the mRNAs for *UBIQUITIN 5* and *ACTIN*. Values are means ± SD of three biological replicates, each with three technical replicates. Statistical analyses were performed using Student's *t*-test. Asterisks denote statistically significant differences (**$P < 0.01$). (*C*) RNA-seq volcano plot showing differentially expressed rice *NLR* genes. A complete list of transcript IDs detected is shown in the raw data file (Raw data for Fig. 6*C*). Cut-off criteria for data in *A* and *C*: $\log_2$[*osrbl3b Myc-Xa21*^{H}/ *Myc-Xa21*^{H}] ≥ 1 and ≤ −1 and *FDR*-value <0.05.

lesser fitness cost than that of *Xoo*, allowing selection of this important *R* gene in the wild species (48).

Mutations leading to loss of OsRBL3b function caused markedly increased accumulation of XA21 protein, which coincided with dehiscence defects, the upregulation of 66 *NLR* genes, and the downregulation of nine JA-responsive and JA-signaling genes, including *OsCOI1a*, in the absence of *Xoo*. The question of whether such upregulation of *NLRs* directly influences fertility remains to be addressed. The suppression of phytohormone-related genes during anthesis is intriguing, because JA-mediated signaling is crucial for anther dehiscence and grain set in plants (49). In addition, rice *COI1* genes (*OsCOI1a* and *OsCOI1b*) are required for JA signaling and JA-induced growth inhibition (50). However, the observed changes in these responsive and signaling genes may be independent of the changes in JA levels, since our RNA-seq analysis shows that no significant enrichment of altered expression

of JA biosynthesis and transport related genes in the sterile *osrbl3b-b Myc-Xa21*^{H} spikelets compared to the fertile *Myc-Xa21*^{H} spikelets at anthesis (*SI Appendix,* Fig. S10). Moreover, key JA biosynthetic genes (e.g., *OsDAD1*, *OsLOX1*, *OsAOS1*, and *OsOPR7*) were not differentially expressed between *osrbl3b-b Myc-Xa21*^{H} and *Myc-Xa21*^{H}. Further studies are required to understand the mechanism and biological significance of the altered gene expression in relation to the observed fertility defects.

OsRBL3b shares 75.2% amino acid identity with OsRBL3a, making it the most closely related protein in the RhoA1 subfamily (*SI Appendix,* Fig. S2). The duplication of OsRBL3a and OsRBL3b might have occurred before speciation in *Oryza* and possibly in the ancestor of rice and cereal crops. The expression patterns of their genes largely differ, with *OsRBL3a* preferably expressed in roots, which can be attributed to the low DNA sequence identity (40.4%) of their promoter regions (*SI Appendix,* Fig. S4 and Dataset S3). This difference in expression sites might contribute to functional variations between these two rhomboid genes. Furthermore, we have shown that OsRBL3b can cleave XA21 and five additional Arabidopsis TMD proteins (*SI Appendix,* Fig. S8*D*), suggesting that this rhomboid protease possesses potentially broad enzymatic ability to cleave TMD proteins. In contrast, OsRBL3a is unable to efficiently cleave XA21. We are uncertain whether OsRBL3a can directly cleave any substrates. In *Drosophila*, cleavage of the membrane protein Spitz by Rhomboid1 requires a third protein, called Star, that traffics Spitz to the compartment where Rhomboid1 is localized (51). Therefore, multiple mechanisms, such as spatiotemporal expression, subcellular localization, and protease–substrate interactions, might all regulate rhomboid cleavage in vivo.

Six of the seven rice *RhoA1* genes showed overlapping but distinct spatiotemporal expression profiles (*SI Appendix,* Fig. S4), suggesting that members of this family might form a proteostasis network that regulates distinct biological processes during development. Certain rhomboids can hydrolyze not only their substrates but also nonsubstrates when a single proline residue is artificially introduced into their TMDs (38). Given the high prevalence of TMD proteins in the cell (approximately 20 to 30% of the proteomes of most eukaryotic organisms) (52), TMD-containing genes that are related to immunity defects and pathological conditions in plants could be edited to contain helix breaking residues to make them for cleavage by specific rhomboid protease(s).

In addition to *OsRBL3b*, low temperatures [28/24 °C (light/dark)] markedly influence the manifestation of reduced grain set in the *osrbl3b Myc-Xa21*^{L} lines (Fig. 4). This indicates that the grain phenotypes can be impacted by an interplay between environmental conditions and XA21 levels. *N. benthamiana* plants are often grown under even lower temperatures [i.e., 24/21 °C (light/dark)] (53), at which XA21 can still be efficiently cleaved by OsRBL3b (Fig. 2). These findings suggest the low-temperature treatment might have a limited effect, if any, on OsRBL3b-mediated cleavage of XA21. Instead, low temperatures are more likely to influence grain set through heightening the competence/effectiveness of XA21 signaling, as proposed previously (13).

Other immune receptors are also subject to fitness and defense balancing. The rice blast resistance gene *PigmR*, which encodes an NLR receptor, has a negative effect on grain weight, although the mechanism underlying the fitness costs is unknown (54). In a naturally occurring disease-resistant line, *PigmR*-mediated yield loss is dampened by *PigmS*, a pollen and panicle-expressed member of the *Pigm* gene family whose product (PigmS) does not prompt disease resistance and is capable of attenuating PigmR homodimerization. In *N. benthamiana*, the NLR modulator NRCX (NLR-REQUIRED FOR CELL DEATH MEMBER X), an atypical NLR protein, is involved in mitigating growth suppression and autoimmune cell death caused by other members of the NRC family (55). Unlike OsRBL3b, which may have arisen from an ancient surveillance system, the NLR modulators have most likely evolved to protect host physiology from immune receptors.

Another interesting aspect is that male-sterile plants form the basis of hybrid breeding for high yields in crops (56). While *osrbl3b-b Myc-Xa21*^{H} is completely sterile during all growth seasons, the *osrbl3b Myc-Xa21*^{L} mutants with lower levels of XA21 are capable of producing at least some grains (Fig. 4). A thorough understanding of the regulation and signaling underlying XA21-induced sterility could aid development of male-sterile as well as fertility-restored plants for a more efficient, two-line breeding system.

We originally identified *OsRBL3b* as an XA21-dependent, differentially up-regulated gene in rice leaves after severe drought stress treatment (Dataset S1). This raises the question of whether *Xoo* exploits *OsRBL3b* to lower XA21 abundance and immunity as the proliferation of the bacterium in the xylem vessels can also cause water-deficit stress. Since XA21 action largely restricts the bacterial population in the infected leaves (9), the severity of the water-deficit stress during incompatible interactions may not be high enough to elevate the transcript level of *OsRBL3b* significantly. In our previous microarray studies, *OsRBL3b* was not identified as a differentially expressed gene in *Myc-XA21*^{H} leaves at 0, 4, 8, 24, 72, and 120 h post inoculation with the incompatible *Xoo* strain PXO99A (~1 cm leaf tissue collected from the inoculated sites) compared to the mock inoculation (57). However, when treated with 13% (w/v) polyethylene glycol (PEG), a chemical that can mimic the effects of drought stress, XA21 seedlings display compromised resistance to PXO99A, suggesting that severe drought stress may suppress XA21 function, although the abundance of XA21 under the stress condition remains to be determined (58). In addition, any roles of *OsRBL3b* in drought response or *Xa21*-mediated drought tolerance remains to be determined experimentally. We cannot exclude the possibility that OsRBL3b-mediated cleavage in leaves plays a positive role in activating drought responsive signaling through releasing a regulator(s) (e.g., XA21IKD or XA21 binding proteins) from the XA21 complex. In human A431 cells (an epidermoid carcinoma cell line expressing high levels of EGFR), the rhomboid protease RHBDL2 can cleave EGFR, leading to the accumulation of the cell-associated EGFR IKD in the nucleus (59).

Rice is a staple food for more than half of the human population, represents 50% of the agronomic biomass produced worldwide, and serves as an important model for cereal crops, including rice, maize, wheat, and sorghum (60, 61). In plants, deployment of *R* genes is an effective and environmentally friendly strategy to control diseases and to stabilize yield performance in crops. However, fitness costs incurred by the expression of various *R* genes have been observed in plants (6, 7, 54, 62). Unlike the *Xa21* gene, *OsRBL3b* orthologs are widely present in rice and other plant species, where they may cleave additional RLKs proteins. Differential expression of *OsRBL3b* to spatiotemporally fine-tune the abundance of XA21 might represent a mechanism by which rice solves the survival-or-reproduction dilemma.

Materials and Methods

Methods are described in more detail in *SI Appendix*.

Plant Materials and Growth Conditions. Rice (*Oryza sativa* L.) ssp. *japonica* cv. Taipei 309 (TP309) was used to generate all transgenic lines in this study. Germination of rice seeds and growth of plants were as described (23). *Nicotiana benthamiana* plants were grown under low temperature conditions [24/21 °C (light/dark)] as described previously (53).

Identification of the *OsRBL3b* Gene and RNA-seq Analysis. *OsRBL3b* was an upregulated gene identified from a comparison of the transcriptomes of previously characterized plants expressing *Myc-XA21-FLAG* (B7-12) (23) and the vector control (A36) under water-deficit stress conditions by RNA-seq analysis as described in *SI Appendix*. To identify DEGs between the sterile *osrbl3b-b Myc-Xa21*^{H} and fertile *Myc-Xa21*^{H} lines, spikelets at anthesis from five plants were harvested from each line and pooled to minimize individual variation. RNA-seq was performed as described in *SI Appendix*.

Phylogenetic and Sequence Analyses of Plant Rhomboid Proteases. OsRBL3b homologs were identified through BLASTp. Phylogenetic analysis of the OsRBL3b homologs across multiple representative plant species was performed using the maximum likelihood (ML) algorithm implemented in IQ-TREE (63) as described in *SI Appendix*. The robustness of the tree topology was assessed by calculating bootstrap support with 1,000 replicates.

Protein or DNA sequence comparisons were performed using EMBOSS Water (https://www.ebi.ac.uk/jdispatcher/psa/emboss_water).

RT-qPCR Analysis. qPCR was performed as described in *SI Appendix* using a LightCycler 480 System (Roche, Indianapolis, IN) according to the manufacturer's instructions under the following conditions: 95 °C, 2 min; (45 cycles of 95 °C, 5 s; 60 °C, 20 s), and 72 °C, 5 min.

Plasmid Constructs. All constructs used in this study are described in *SI Appendix* and have been verified by DNA sequencing. All primers used in this study are listed in Dataset S6.

Rhomboid Cleavage of XA21 in *N. benthamiana*. Infiltration of *N. benthamiana* with *Agrobacterium* strain EHA105 harboring a construct designed for transient gene expression was performed as previously described (64) and detailed in *SI Appendix*.

Immunoblot Analysis of Rice Samples. Immunoblot analysis was performed as described previously (14) and detailed in *SI Appendix*. Quantification of protein levels on the blots and the subsequent statistical analysis were carried out as described by Wang et al. (65).

Generation of Rice *osrbl3b* Mutants by the CRISPR/Cas9 System. Homozygous *osrbl3b* mutant plant lines *osrbl3b-1* (p.Trp111ThrfsTer121) and *osrbl3b-2* (p.Asp112GlufsTer116) were generated in TP309 using CRISPR/Cas9 as described in *SI Appendix*. The biallelic mutant line *osrbl3b-b* [p.(Trp111ThrfsTer121);(Asp112GlyfsTer116)] were made in line 4021-3 (containing the *Myc-Xa21*^{H} and *hptII* genes). All CRISPR mutants in this study were annotated using full Human Genome Variation Society (HGVS) nomenclature.

Subcellular Localization of OsRBL3b Using Rice Protoplasts. Sixteen hours after transfection with DNA constructs of interest, the protoplasts were visualized using a Zeiss LSM800 or a Leica TCS SP5 confocal laser scanning microscope or a Keyence All-in-One BZ-X800 Fluorescence Microscope (*SI Appendix*). FM4-64 staining was performed by incubating the dye (final concentration, 10 μM) with transfected protoplasts for 10 min at room temperature. eGFP and FM4-64 were excited with the 488–nm laser line. Fluorescence emissions were captured at 410 to 535 nm for eGFP and 650 to 700 nm for FM4-64. Images were analyzed using ZEN 2.0 software. Multiple transfected cells were inspected with three representative cells being shown. The experiment was repeated three times.

***Xoo* Inoculation.** The incompatible *Xoo* strain PXO99^{A} was used to inoculate 2-wk-old rice seedlings (*SI Appendix*) using the leaf-clipping method (13).

Spikelet Fertility, Pollen Viability, and Anther Dehiscence Assays. Spikelet fertility, pollen viability, and anther dehiscence assays were detailed in *SI Appendix*.

Alkaline Phosphatase (AP)-TMD Shedding Assay. Stable *OsRBL3b* and *OsRBL3b*^{S187A} cell lines were generated by transfecting the *pcDNA3.1-OsRBL3b* and *pcDNA3.1-OsRBL3b*^{S187A}constructs (see above) into HEK293 cells (ATCC, Manassas, VA), respectively, following by selecting with G418 (500 ng/mL) for 3 wk. Stable clones were expanded as individual cell lines and maintained in DMEM supplemented with 10% fetal bovine serum (FBS) and 1 × antibiotic-antimycotic solution (ThermoFisher Scientific). AP-TMD shedding assays were performed in 96-well plates as described (22) and detailed in *SI Appendix*. The experiment was repeated two times.

Quantification and Statistical Analysis. Quantification of Western blots was performed using ImageJ. Volcano plots were generated using SRPLOT (https://www.bioinformatics.com.cn/plot_basic_3_color_volcano_plot_086_en). One-way ANOVA tests were performed to compare multiple groups of data, and Student's *t*-tests were carried out to compare two independent groups of data.

Data, Materials, and Software Availability. All study data are included in the article and/or supporting information.

ACKNOWLEDGMENTS. We thank Dr. Kvido Strisovsky, Dr. Dean Gabriel, and Anita K. Snyder for critical reading of the manuscript; Drs. Frank White, Shiyong Song, and Lizi Wu for invaluable discussion; Dr. Shamsunnaher, Grace Marten, Yoan Argote, Lijing Chen, Zhenqiang Lu, Yi Shen, Dr. Zhukuan Cheng for technical assistance; Drs. Adam G. Grieve and Matthew Freeman for the pcDNA3.1_TMDscreen vector; Dr. Shin-Han Shiu for providing rice RLK sequences; Dr. Pamela Ronald for providing the 4021-3 line, Dr. Yinong Yang for the pC1300S binary vector; Dr. Zuhua He for the *GFP* construct and high school teachers Shelby Ball, Kate Cafee, Rose Hess, Patrick Kelly, and Wanda Rosario for independently verifying the impaired anther dehiscence in the *osrbl3b Myc-Xa21* mutants. Special thanks to Dr. Nian Wang for invaluable support. The work was supported by the NSF (no. 2114833 to W.-Y.S.), the USDA National Institute of Food and Agriculture (no. 2015-67013-22910 to S.C., K.E.K., and W.-Y.S.), the Intramural Research Program of the National Institute of Environmental Health Sciences (ZIC ES103371 to J.-L.L.), and funds from the UF-Department of Plant Pathology and the UF-IFAS Dean's office.

Author affiliations: [a]Department of Plant Pathology, Institute of Food and Agricultural Sciences, University of Florida, Gainesville, FL 32611; [b]Integrative Bioinformatics, National Institute of Environmental Health Sciences, NIH, Research Triangle Park, NC 27709; [c]Centro de Tecnologia Canavieira Genomics, Saint Louis, MO 63132; [d]Department of Molecular Genetics and Microbiology, University of Florida, Gainesville, FL 32611; [e]Department of Bioinformatics and Molecular Biology, College of Life Sciences, Hebei Agricultural University, Baoding, Hebei 071001, P. R. China; [f]Emerging Pathogens Institute, University of Florida, Gainesville, FL 32610; [g]Department of Pathology and Laboratory Medicine, Tulane University, New Orleans, LA 70112; [h]Department of Biology, University of Mississippi, Oxford, MS 38677; [i]Department of Biology, Genetics Institute, University of Florida, Gainesville, FL 32611; and [j]Horticultural Sciences Department, IFAS, University of Florida, Gainesville, FL 32611

Author contributions: S.V., X.H., L.P., S.C., K.E.K., and W.-Y.S. designed research; S.V., X.H., G.Z., B.d.T.F., X.-X.W., J.N., J.C.H. T., A.P., X.C., D.L., W.-M.X., S.D., G.-z.L., L.P., and W.-Y.S. performed research; S.V., X.H., J.-L.L., J.C.H. T., R.S., E.M.G., L.P., and W.-Y.S. analyzed data; X.H. wrote the sections related to the genetic crossing between the lines and the *Pigm* gene; and W.Y.S. and S.V. cowrote the rest of the manuscript with input from other authors.

The authors declare no competing interest.

This article is a PNAS Direct Submission.

[1]S.V. and X.H. contributed equally to this work.

[2]Present address: Department of Plant Pathology, Citrus Research and Education Center, Institute of Food and Agricultural Sciences, University of Florida, Lake Alfred, FL 33850.

[3]Present address: Jiangsu Institute of Agricultural Sciences in Coastal Area, Jiangsu 224001, P.R. China.

1. J. D. Jones, J. L. Dangl, The plant immune system. *Nature* **444**, 323–329 (2006).
2. P. C. Ronald, B. Beutler, Plant and animal sensors of conserved microbial signatures. *Science* **330**, 1061–1064 (2010).
3. D. Couto, C. Zipfel, Regulation of pattern recognition receptor signalling in plants. *Nat. Rev. Immunol.* **16**, 537–552 (2016).
4. J. M. Zhou, Y. Zhang, Plant immunity: Danger perception and signaling. *Cell* **181**, 978–989 (2020).
5. J. D. Jones, R. E. Vance, J. L. Dangl, Intracellular innate immune surveillance devices in plants and animals. *Science* **354**, aaf6395 (2016).
6. D. Tian, M. B. Traw, J. Q. Chen, M. Kreitman, J. Bergelson, Fitness costs of *R*-gene-mediated resistance in *Arabidopsis thaliana*. *Nature* **423**, 74–77 (2003).
7. T. L. Karasov *et al.*, The long-term maintenance of a resistance polymorphism through diffuse interactions. *Nature* **512**, 436–440 (2014).
8. G. S. Khush, E. Bacalangco, T. Ogawa, A new gene for resistance to bacterial blight from *O. longistaminata*. *Rice Genet. Newsl.* **7**, 2 (1990).
9. W. Y. Song *et al.*, A receptor kinase-like protein encoded by the rice disease resistance gene, *Xa21*. *Science* **270**, 1804–1806 (1995).

10. R. N. Pruitt *et al.*, The rice immune receptor XA21 recognizes a tyrosine-sulfated protein from a Gram-negative bacterium. *Sci. Adv.* **1**, e1500245 (2015).
11. R. N. Pruitt *et al.*, A microbially derived tyrosine-sulfated peptide mimics a plant peptide hormone. *New Phytol.* **215**, 725–736 (2017).
12. X. Chen *et al.*, An XA21-associated kinase (OsSERK2) regulates immunity mediated by the XA21 and XA3 immune receptors. *Mol. Plant* **7**, 874–892 (2014).
13. Q. Chen, X. Chen, Shamsunnher, W. Y. Song, Reversible activation of XA21-mediated resistance by temperature. *Eur. J. Plant Pathol.* **153**, 1177–1184 (2019).
14. W. H. Xu *et al.*, The autophosphorylated Ser686, Thr688, and Ser689 residues in the intracellular juxtamembrane domain of XA21 are implicated in stability control of rice receptor-like kinase. *Plant J.* **45**, 740–751 (2006).
15. C. J. Park, P. C. Ronald, Cleavage and nuclear localization of the rice XA21 immune receptor. *Nat. Commun.* **3**, 920 (2012).
16. M. Antolin-Llovera, M. K. Ried, M. Parniske, Cleavage of the SYMBIOSIS RECEPTOR-LIKE KINASE ectodomain promotes complex formation with Nod factor receptor 5. *Curr. Biol.* **24**, 422–427 (2014).
17. E. K. Petutschnig *et al.*, A novel Arabidopsis CHITIN ELICITOR RECEPTOR KINASE 1 (CERK1) mutant with enhanced pathogen-induced cell death and altered receptor processing. *New Phytol.* **204**, 955–967 (2014).
18. A. Dominguez-Ferreras, M. Kiss-Papp, A. K. Jehle, G. Felix, D. Chinchilla, An overdose of the Arabidopsis coreceptor BRASSINOSTEROID INSENSITIVE1-ASSOCIATED RECEPTOR KINASE1 or its ectodomain causes autoimmunity in a SUPPRESSOR OF BIR1-1-dependent manner. *Plant Physiol.* **168**, 1106–1121 (2015).
19. J. Zhou *et al.*, Proteolytic processing of SERK3/BAK1 regulates plant immunity, development, and cell death. *Plant Physiol.* **180**, 543–558 (2019).
20. M. Freeman, The rhomboid-like superfamily: Molecular mechanisms and biological roles. *Annu. Rev. Cell Dev. Biol.* **30**, 235–254 (2014).
21. S. Urban, Rhomboid proteins: conserved membrane proteases with divergent biological functions. *Genes Dev.* **20**, 3054–3068 (2006).
22. A. G. Grieve *et al.*, Conformational surveillance of Orai1 by a rhomboid intramembrane protease prevents inappropriate CRAC channel activation. *Mol. Cell* **81**, 4784–4798.e7 (2021).
23. Shamsunnaher *et al.*, Rice immune sensor XA21 differentially enhances plant growth and survival under distinct levels of drought. *Sci. Rep.* **10**, 16938 (2020).
24. Q. Li, N. Zhang, L. Zhang, H. Ma, Differential evolution of members of the rhomboid gene family with conservative and divergent patterns. *New Phytol.* **206**, 368–380 (2015).
25. C. J. Park *et al.*, Overexpression of the endoplasmic reticulum chaperone BiP3 regulates XA21-mediated innate immunity in rice. *PLoS One* **5**, e9262 (2010).
26. F. Chen *et al.*, Plasma membrane localization and potential endocytosis of constitutively expressed XA21 proteins in transgenic rice. *Mol. Plant* **3**, 917–926 (2010).
27. S. Song *et al.*, OsFTIP7 determines auxin-mediated anther dehiscence in rice. *Nat. Plants* **4**, 495–504 (2018).
28. A. Chini *et al.*, The JAZ family of repressors is the missing link in jasmonate signalling. *Nature* **448**, 666–671 (2007).
29. B. Thines *et al.*, JAZ repressor proteins are targets of the SCF(COI1) complex during jasmonate signalling. *Nature* **448**, 661–665 (2007).
30. H. Ye, H. Du, N. Tang, X. Li, L. Xiong, Identification and expression profiling analysis of TIFY family genes involved in stress and phytohormone responses in rice. *Plant Mol. Biol.* **71**, 291–305 (2009).
31. D. X. Xie, B. F. Feys, S. James, M. Nieto-Rostro, J. G. Turner, *COI1*: An *Arabidopsis* gene required for jasmonate-regulated defense and fertility. *Science* **280**, 1091–1094 (1998).
32. H. Y. Lee *et al.*, *Oryza sativa* COI homologues restore jasmonate signal transduction in Arabidopsis *coi1-1* mutants. *PLoS One* **8**, e52802 (2013).
33. J. S. Seo *et al.*, OsbHLH148, a basic helix-loop-helix protein, interacts with OsJAZ proteins in a jasmonate signaling pathway leading to drought tolerance in rice. *Plant J.* **65**, 907–921 (2011).
34. K. Kiribuchi *et al.*, *RERJ1*, a jasmonic acid-responsive gene from rice, encodes a basic helix-loop-helix protein. *Biochem. Biophys. Res. Commun.* **325**, 857–863 (2004).
35. X. Liu, X. Bai, X. Wang, C. Chu, OsWRKY71, a rice transcription factor, is involved in rice defense response. *J. Plant Physiol.* **164**, 969–979 (2007).
36. Y. He *et al.*, Jasmonic acid plays a pivotal role in pollen development and fertility regulation in different types of P(T)GMS rice lines. *Int. J. Mol. Sci.* **22**, 7926 (2021).
37. L. Wang *et al.*, Large-scale identification and functional analysis of *NLR* genes in blast resistance in the Tetep rice genome sequence. *Proc. Natl. Acad. Sci. U.S.A.* **116**, 18479–18487 (2019).
38. S. M. Moin, S. Urban, Membrane immersion allows rhomboid proteases to achieve specificity by reading transmembrane segment dynamics. *Elife* **1**, e00173 (2012).
39. S. D. Clouse, M. Langford, T. C. McMorris, A brassinosteroid-insensitive mutant in *Arabidopsis thaliana* exhibits multiple defects in growth and development. *Plant Physiol.* **111**, 671–678 (1996).
40. J. Li, J. Chory, A putative leucine-rich repeat receptor kinase involved in brassinosteroid signal transduction. *Cell* **90**, 929–938 (1997).
41. J. Li *et al.*, BAK1, an Arabidopsis LRR receptor-like protein kinase, interacts with BRI1 and modulates brassinosteroid signaling. *Cell* **110**, 213–222 (2002).
42. K. H. Nam, J. Li, BRI1/BAK1, a receptor kinase pair mediating brassinosteroid signaling. *Cell* **110**, 203–212 (2002).
43. J. Liu, J. Li, L. Shan, SERKs. *Curr. Biol.* **30**, R293–R294 (2020).
44. E. P. B. Fontes, SERKs and NIKs: Coreceptors or signaling hubs in a complex crosstalk between growth and defense? *Curr. Opin. Plant Biol.* **77**, 102447 (2024).
45. D. Chinchilla *et al.*, A flagellin-induced complex of the receptor FLS2 and BAK1 initiates plant defence. *Nature* **448**, 497–500 (2007).
46. Y. Cao *et al.*, The kinase LYK5 is a major chitin receptor in Arabidopsis and forms a chitin-induced complex with related kinase CERK1. *Elife* **3**, e03766 (2014).
47. S. Tong, M. Ashikari, K. Nagai, O. Pedersen, Can the wild perennial, rhizomatous rice species *Oryza longistaminata* be a candidate for *de novo* domestication? *Rice (N Y)* **16**, 13 (2023).
48. C. Tekete *et al.*, Characterization of new races of *Xanthomonas oryzae* pv. *oryzae* in mali informs resistance gene deployment. *Phytopathology* **110**, 267–277 (2020).
49. Z. A. Wilson, J. Song, B. Taylor, C. Yang, The final split: The regulation of anther dehiscence. *J. Exp. Bot* **62**, 1633–1649 (2011).
50. D. L. Yang *et al.*, Plant hormone jasmonate prioritizes defense over growth by interfering with gibberellin signaling cascade. *Proc. Natl. Acad. Sci. U.S.A.* **109**, E1192–E1200 (2012).
51. B. Z. Shilo, Developmental roles of rhomboid proteases. *Semin. Cell Dev. Biol.* **60**, 5–9 (2016).
52. A. Krogh, B. Larsson, G. von Heijne, E. L. Sonnhammer, Predicting transmembrane protein topology with a hidden Markov model: Application to complete genomes. *J. Mol. Biol.* **305**, 567–580 (2001).
53. S. Vergish, R. Wolf, W. Y. Song, Simplified protocol to demonstrate gene expression in *Nicotiana benthamiana* using an *Agrobacterium*-mediated transient assay. *Bio Protoc.* **14**, e4987 (2024).
54. Y. Deng *et al.*, Epigenetic regulation of antagonistic receptors confers rice blast resistance with yield balance. *Science* **355**, 962–965 (2017).
55. H. Adachi *et al.*, An atypical NLR protein modulates the NRC immune receptor network in *Nicotiana benthamiana*. *PLoS Genet.* **19**, e1010500 (2023).
56. L. Chen, Y. G. Liu, Male sterility and fertility restoration in crops. *Annu. Rev. Plant Biol.* **65**, 579–606 (2014).
57. Q. Gan *et al.*, Transcriptional characteristics of *Xa21*-mediated defense responses in rice. *J. Integr. Plant Biol.* **53**, 300–311 (2011).
58. X. Zhang, W.-Y. Song, Drought treatment: A new tool for dissecting XA21 signaling in rice. *J. Exp. Mol. Pathol.* **1**, 1–4 (2022).
59. H. J. Liao, G. Carpenter, Regulated intramembrane cleavage of the EGF receptor. *Traffic* **13**, 1106–1112 (2012).
60. M. Sticklen, Plant genetic engineering to improve biomass characteristics for biofuels. *Curr. Opin. Biotechnol.* **17**, 315–319 (2006).
61. R. A. Wing, M. D. Purugganan, Q. Zhang, The rice genome revolution: From an ancient grain to Green Super Rice. *Nat. Rev. Genet* **19**, 505–517 (2018).
62. Z. Hao, J. Wang, L. P. Wang, R. X. Tao, Influences of the disease resistance conferred by the individual transgenes, *Pi-d2*, *Pi-d3* and *Xa21*, on the transgenic rice plants in yield and grain quality. *Afr. J. Biotechnol.* **8**, 4 (2009).
63. B. Q. Minh *et al.*, IQ-TREE 2: New models and efficient methods for phylogenetic inference in the genomic era. *Mol. Biol. Evol.* **37**, 1530–1534 (2020).
64. X. Huang, X. Liu, X. Chen, A. Snyder, W. Y. Song, Members of the XB3 family from diverse plant species induce programmed cell death in *Nicotiana benthamiana*. *PLoS One* **8**, e63868 (2013).
65. W. Wang, J. Kim, T. S. Martinez, E. Huq, S. Sung, COP1 controls light-dependent chromatin remodeling. *Proc. Natl. Acad. Sci. U.S.A.* **121**, e2312853121 (2024).